

# Thermography detection of hidden defects

E.M. Sheregii

Center for Microelectronics and Nanotechnology

University of Rzeszow

S. Pigoia str. 16, 35-959 Rzeszow

POLAND

sheregii@ur.edu.pl <http://www.nanocentrum.ur.edu.pl>

*Abstract:* - Thermography measurements allow to detect the defects that may appear undersurface of details with protecting covering. Subsurface defects in the sample have been detected using the high resolution thermal imaging camera FLIR SC7000. To introduce additional energy in a researched sample, a scanning hot air (about 110°C) nozzle is applied (a patent application P.403346). The hidden defect causes a temperature increase in comparison with the remaining area what is a result of changes in emissivity. The results are compared with the pulse thermography method using the xenon lamp for excitation.

*Key-Words:* - thermography, defects, scanning, noninvasive control

## 1 Introduction

The intensity of radiation emitted by the surface in the entire spectral range depends on the surface temperature what makes the detection of this radiation the basis for the non-contact method of the temperature measurement [1]. The research development based on the IR thermography to detect defects in the surface layer of materials has been observed in the last years. Thermography offers noncontact, wide area detection of subsurface defects, and can be used as an alternative or the complement to the conventional inspection technologies [2-7].

The essence of this research is the thermal response analysis of the material stimulated by the external heat impulse. After supplying specified quantity of energy to the material, for example in the form of a heat pulse, the thermal front begins to move into the material due to the thermal diffusion. The presence of areas containing defects with thermal properties different from areas without defects, causes a change in the diffusion rate what enables to observe the defects location analyzing the temperature distribution on the researched sample surface. [2,5] On the other hand, the size of the detected defects using the pulse thermography method should be not less than few millimeters if a whole surface (usually the macroscopic one) of the researched sample is stimulated [7]. Nevertheless, that is excellent method for express-control of macroscopic specimens.

Other methods of excitation can be used in the thermography detected defects, namely ultrasounds.

The ultrasound thermography is used as the interaction between mechanical and thermal waves to detect material defects. If some damage in components absorbs the excitation of high energy ultrasound waves then it is locally heated. The resulting temperature gradient is captured by an infrared camera on the sample surface. This method is suitable for the applications in the cracks detection, adhesion testing and welded joints. It is possible to detect delamination and impact damage in materials using the ultrasound method [8,9].

In this paper a specially designed hot air nozzle as an excitation source with scanning on the sample surface is proposed for the noncontact and noninvasive control of subsurface defects [10]

## 2 Basic theory

### 2.1 Fourier equation

Heat diffusion through a solid is a complex 3D problem that can be described by the Fourier's law of the heat diffusion or the heat equation [11]. The 1D solution of the Fourier equation for the propagation of a Dirac heat pulse, i.e. an ideal waveform defined as an intense unit-area pulse in a semi-infinite isotropic solid, has the form [12, 13]:

$$T(t) = T_0 + Q/e(\pi t)^{1/2} \quad (1)$$

where  $Q$  is the energy absorbed by the surface and  $T_0$  is the initial temperature,  $e$  is the effusivity:

$$e = (k \rho c)^{1/2} \quad (2)$$

which is a thermal property that measures the material ability to exchange heat with its surroundings and is an important parameter in this method.

## 2.2 Role of effusivity

If the properties of material ( $k$ ,  $\rho$ ,  $c_p$ ) are changed, the effusivity  $e$  is changed too, what causes the local change of temperature  $\Delta T$ . The time of this change is connected with another parameter – the thermal diffusivity  $\alpha$ . Any change in the sample temperature is related to the thermal diffusivity  $\alpha$  [11],

$$\alpha = k/\rho c \quad (3)$$

where  $k$  is the thermal conductivity,  $\rho$  is the density and  $c$  is the heat capacity at the constant pressure. That is the second very important parameter in the proposed method. The relation between these two parameters ( $e$  and  $\alpha$ ) enables to choose the optimal velocity  $v$  for scanning of the hot spot as well as the minimal value of the  $\Delta T$  necessary to detect a hidden defect.

## 3 Experiment

### 3.1 Material and methods

A scanning hot air nozzle is mounted on a stationary platform with a high resolution thermal imaging camera FLIR SC7000 (IR camera). The heat flow is directed to the surface of the sample which is placed on the table moving with the selected speed in the direction of  $z$  axis (see Fig. 1 a,b). The air pressure getting out of the nozzle was 0.2 MPa. The temperature of hot air was 110°C.

Thermography is based on the radiation emission of the objects. Therefore, the emission coefficient  $\varepsilon = E/E_s$  as the ratio of emissivity  $E$  of a real body to the emissivity  $E_s$  of the absolute black body at the same temperature, is important, particularly in the case of the metallic researched surface. It is caused by a small value of the emissivity in comparison with the reflectivity. So, the precise determination of the emission coefficient  $\varepsilon$  has a principal meaning for the temperature correct measurement.

The IR camera used in this work is operating in the short wave region at 3-5 $\mu$ m. To perform correct measurements of the temperature distribution on the surface, a series of the IR

camera settings were made. That is a verification of few parameters for example: emissivity of the object and the distance (this parameter is important because a big part of radiation of the object is absorbed in the air so the distance was 0.5m). On the other hand this distance influences the spatial resolution of the IR camera, which is expected to be maximum. The sample with dimensions 60mm x 20mm x 5mm was made from C45 steel and contained specially created defects in the form of 5 holes on the back side of a sample with a different size of diameters: 6mm, 5mm, 4mm, 3mm, 2mm. The depth of holes is equal to two thirds of the thickness. Front and back sides of the sample are shown in Fig. 2 a,b. The scale is shown in Fig. 2c in order to state the positions of holes on the back side.

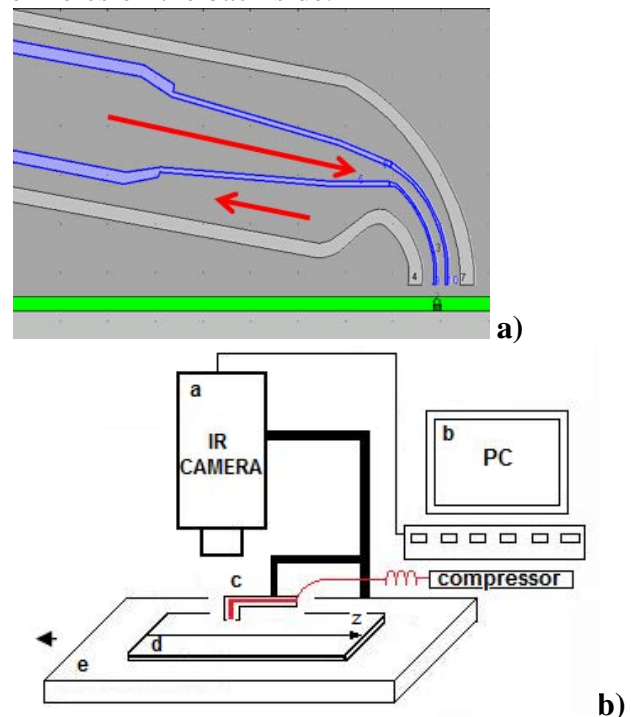


Fig. 1. a) A hot air nozzle: hot air is getting from the nozzle of 0.4 mm diameter (blue color) and sucks up the air reflected from the investigated surface (white color); b) Scheme of experiment.

In order to perform precise motion sequences of the sample a motorized positioning system such as an OWIS PKTM 70 table movable in the  $x$ ,  $y$ ,  $z$  directions, was used. The positioning system enables to choose very precisely the velocity of the sample motion  $v$ .

### 3.2 Choosing of parameters

The velocity value is important from the point of view of the defect detection because the heat

diffusion length  $L_H = \sqrt{\alpha\tau}$  is determined by the thermal diffusivity  $\alpha$  (see the previous chapter) and the next inequality should be fulfilled:

$$d > L_H \quad (4)$$

where  $d$  is the size of the defect and  $\tau$  is the time of the nozzle going along the defect area:

$\tau = d/v$ . The equation (4) means that the time  $\tau$  is less than the heat diffusion time on the same distance. Therefore, the nozzle velocity is limited by minimum

$$v > \frac{\alpha}{d} \quad (5)$$

On the other hand, this velocity has a top limit also because it is necessary to register the defect using the change of temperature  $\Delta T = Q/e(\pi t)^{1/2}$  as it was shown on the equation (1). The top limit for the nozzle velocity depends on the minimal  $Q$  value necessary for the efficient temperature change in the defect area, simultaneously the effusivity also influences the  $\Delta T$  increase. Thus, the nozzle velocity maximum depends on the material parameters of the examined sample and on the  $Q$  value delivered by the nozzle. The last one can be derived from the nozzle velocity  $v$ , the hot air temperature  $T_{air}$  and the hot air flux velocity  $V_{air} = \Delta V/\Delta t$  ( $\Delta V$  is the volume of the hot air getting out from the nozzle during the time interval  $\Delta t$ ), namely:

$$Q = c_{air}\rho_{air}d(T_{air}-T_0)V_{air}/v \quad (6)$$

where  $c_{air}$  and  $\rho_{air}$  are the hot air heat capacity and the hot air density, respectively.

The best nozzle velocity  $v$  selected during the measurement conditions was equal to 4.8mm/s. (at the same time it is the speed of the OWIS PKTM 70 table).

The measurement consisted of the registration of the radiation intensity  $I$  as a function of the coordinate  $z$  value at scanning the sample surface along the  $z$  axis by the hot air nozzle. The FLIR SC7000 camera registered the radiation generated by the heat trace during the scanning. The region on the surface of the heat trace is possible to be selected by the Altair software and the signal intensity associated with this region of a sample is displayed by this computer program after choosing the area of the heat trace. Thus, the registered magnitude  $I(z)$  is the radiation intensity generated by the selected area on the heat trace.

### 3.3 Results

In Figs. 3 and 4 are presented the experimental curves of  $I(z)$  obtained at the above described experiment conditions. In Fig. 3a,b are presented the  $I(z)$ -curves obtained during scanning along the red line where the row of the holes is placed on the back side of the sample (see Figs. 2a,b). The  $I(z)$ -curve in Fig. 3a was registered using the heat trace region shown in the insert. It can be seen that the  $I(z)$ -curve displays the maxima corresponding to the increased temperature in the area at the positions of defects (holes shown in Fig. 2b).

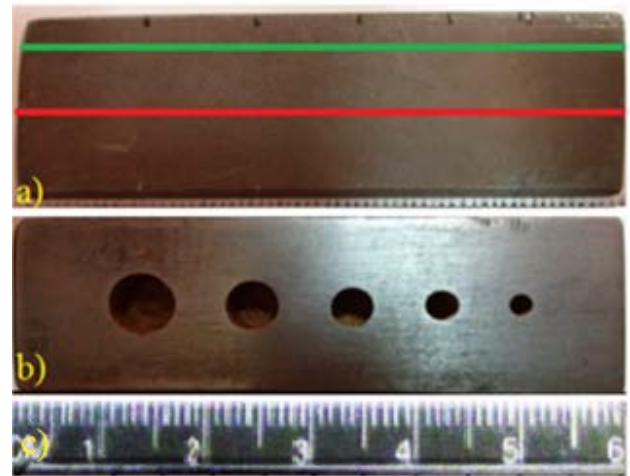


Fig.2 Picture of the sample: a ) front size, b) back size, c) scale.

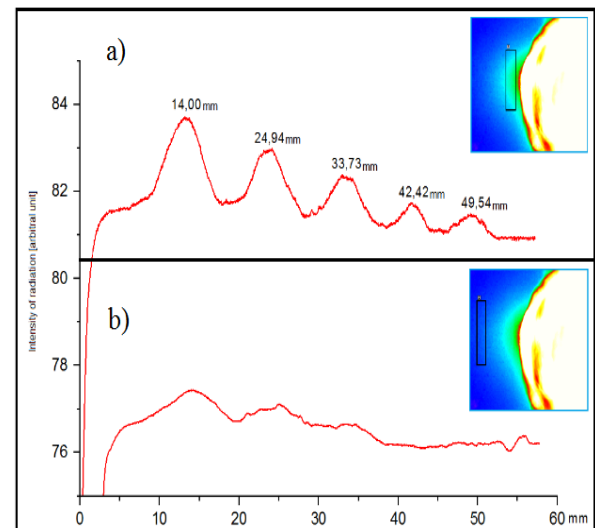


Fig. 3 The  $I(z)$ -curves obtained at scanning along the red line (see Fig. 2a): a) using the radiation from the region of the heat track, shown in insert; b) using the radiation from the region out of the heat track, shown in insert also.

Whereas, in case of the  $I(z)$ -curve obtained by using the IR-signal from the region *out of the heat trace* (see Fig. 3b), the intensity of the maxima at the positions of the largest holes are much smaller and no maxima are observed at the positions of the last two holes.

It means that the detection of the hidden defects depends on the selected area which is the source of the IR-signal, namely: this area should belong to the heat trace caused by the nozzle.

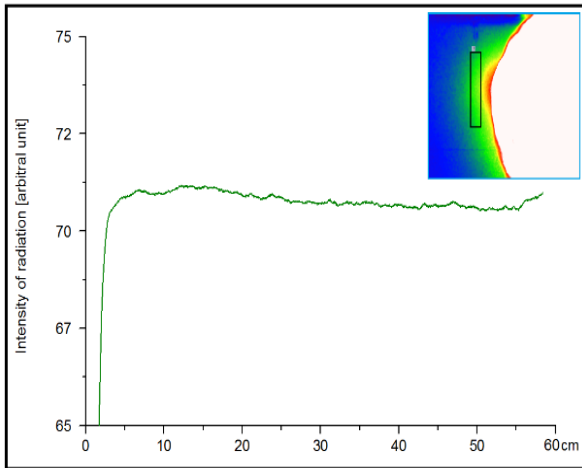


Fig. 4. The  $I(z)$ -curve obtained at scanning along the green line (see Fig.2a) using the radiation from the region of the heat trace, shown in insert

In the Fig. 4 is shown the  $I(z)$ -curve obtained during scanning along the green line (see Fig. 2a) which is out of the holes row. No maxima are displayed on this curve.

### 3.4 Discussion

In order to compare the results obtained using a hot air nozzle, the impulse of the xenon flash lamp as an excitation source was applied to the same sample. In this experiment the impulse with 6kJ energy and 6ms time generated enough power to register the temperature distribution on the surface of the sample and to visualize hidden defects by the IR camera. [13].

As shown in Fig 5b after the excitation of the sample by the impulse from the xenon flash lamp the IR-camera registered from the back side of a sample only the first three largest holes. The last two smallest holes are invisible using this method. Whereas, scanning by the hot air nozzle allowed to detect all five holes, the minimal size of which was 2 mm.

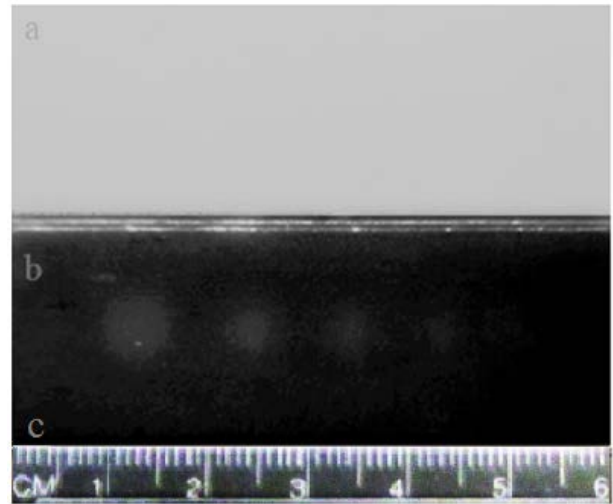


Fig. 5. a) image of the sample back side in the visible region of spectra, b) thermogram of the same surface obtained by the IR-camera after impulse excitation using xenon lamp: three holes are visible clearly, c) scale

Thus, the proposed method of hot spot scanning is more effective for detection of defects smaller than 2 mm. The method described above enables to deliver energy directly to the defect area what causes higher sensitivity in the material ability to exchange heat with its surrounding determined by the thermal effusivity  $e$  (see Eqn. 1).

The Eqn. 1 points out that the highest temperature is in the region where more energy  $Q$  is delivered. If the nozzle is going along the larger defect, according to the Eqn. 6, the  $Q$  is larger too, because one is proportional to  $d$  – size of the defect. The minimal size of the defect detected by this method appears to be worth analyzing. A hidden hole (existing on the back side of another sample) with a diameter of 0.5 mm was detected experimentally. Theoretically, this minimal size can be calculated taking into account maximal sensitivity of the IR-camera to the temperature change  $\Delta T$  at the registration of the radiation intensity from the sample surface.

At the experiment conditions this maximal sensitivity should be 0.1K according to the documentation of the IR-camera. It is expected however, that the hole with a diameter of 0.2 mm could be registered using the proposed method at the conditions of this experiment.

## 4 Conclusion

The thermography method of the hidden defect controlling using the scanning hot spot is developed. The specimen made of C45 steel with flat-bottom holes was prepared. The proposed method of the noncontact and noninvasive control of hidden defects using the scanning hot air nozzle, enables to detect the holes existing on the back side of the steel plate (actually “a hidden defect”) of  $d \leq 2\text{mm}$  size. The alternative noncontact and noninvasive method using the xenon flash lamp impulse as a source of excitation enables to detect the holes on the same steel plate with a diameter size of  $d \geq 3.5\text{mm}$ . Theoretically, the minimal size of such kind of a hidden defect which is possible to be detected using the proposed method, is 0.2 mm what will be verified in the future. Therefore, after application of the impulse thermography method for the macroscopic defect control, the some places where the defects of size less than 2 mm could be presented, should be verified by complementary thermography method using the scanning hot spot.

### References:

- [1] Vollmer M., Möllman K.-P., *Infrared Thermal Imaging*, Wiley-Vch, N-Y, 2010.
- [2] X. Maldague, *Theory and Practice of Infrared Technology for Nondestructive Testing*, John Wiley – Interscience, N-Y, 2001
- [3] Burrows, S. E., Dixon, S., Pickering, S. G., Li, T. and Almond, D. P., *Thermographic detection of surface breaking defects using a scanning laser source. NDT & E International*, Vol. 44, No 7, 2011, pp. 589-596.
- [4] X. Maldague, S. Marinetti, Pulse phase infrared thermography, *J. Appl. Phys.*, Vol. 79 No. 5, 1996, pp. 2694-2698.
- [5] S. Marinetti, Y. A. Plotnikov, W. P. Winfree, A. Braggiotti, Pulse phase thermography for defect detection and visualization, *Proc SPIE* (1999).
- [6] F. C. Sham, C. Nelson, L. Long, Surface crack detection by flash thermography on concrete surface, *Insight*, Vol. 50, 2008 pp.240-243,
- [7] Masashi Ishikawa, Hiroshi Hatta, Yoshio Habuka, Ryo Fukui, Shin Utsunomiya,

Detecting deeper defects using pulse phase thermography, *Infrared Physics & Technology* Vol. 57, No.3, 2013, pp. 42–49.

- [8] Th. Zweschper, A. Dillenz, G. Riegert, G. Busse, *Ultrasound Thermography in NDE: Principle and Applications, Acoustical Imaging* Vol. 27, No. 1, 2004, pp 113-120
- [9] A. Gleiter, Ch. Spießberger, G. Busse, Lockin Thermography with Optical or Ultrasound Excitation, *Journal of Mechanical Engineering*, Vol. 56, No. 10, 2010, pp. 619-624
- [10] K. Maś, M. Woźny, S. Prochorenko, K. Kashpor, E. Sheregii, „Sposób bezdotykowej kontroli jednorodności ochronnych powłok powierzchniowych, nr P.403346
- [11] Carslaw, H.S. and Jaeger, J.C., *Conduction of Heat in Solids*, Clarendon Press: Oxford, 1959.
- [12] M. Pilla, M. Klein, X. Maldague A. Salerno, “New absolute contrast for pulsed thermography” in D. Balageas G. Busse, C. Carlomagno (Eds.), *Proc. QIRT (Quantitative Infrared Thermography)*, Dubrovnik, Croatia, 2002
- [13] O. Wysocka-Fotek, W. Oliferuk, M. Maj “Reconstruction of size and depth of simulated defects in austenitic steel plate using pulsed infrared thermography”, *Infrared Physics & Technology*, Vol. 55, No. 2, 2012, pp. 363 – 367.